A novel polyoxometalate-functionalized mesoporous hybrid silica: synthesis and characterization†

Rongfang Zhang and Chun Yang*

Received 3rd January 2008, Accepted 28th March 2008
First published as an Advance Article on the web 18th April 2008
DOI: 10.1039/b800025e

Novel polyoxometalate (POM)-functionalized mesoporous hybrid silicas, SiW_{11}/MHS, have been synthesized by a co-condensation route and employment of Keggin-type monovacant SiW_{11} as POM precursor in the presence of block copolymer $EO_{20}PO_{70}EO_{20}$ (P123) under acidic conditions. This synthesis allows a bulky inorganic metal–oxygen cluster to be grafted directly on the surface of ordered mesoporous silica with SBA-15 architecture. The as-obtained SiW_{11}/MHS samples were characterized by FT-IR, UV-vis/DRS, ^{29}Si CP MAS NMR, XRD, TEM, N_2 adsorption–desorption measurement and elemental analysis. These materials possess not only hexagonal mesoscopic order and homogeneous pore sizes, but also intact Keggin units immobilized in channels by covalent linkages with the mesopore walls. This covalent bond results from the reaction of TEOS with SiW_{11}, in which Si species are inserted into the vacancy of lacunary SiW_{11} to form Si–O–W bonds and an intermediate $SiW_{11}Si_2$, by which the POM is bound onto the framework of mesoporous silica. Investigation of the synthesis conditions indicates that the quality of the product depends on the initial SiW_{11} concentration, the aging temperature of the sample and the prehydrolysis time of TEOS. A higher SiW_{11} concentration can enhance the loading of SiW_{11} to a certain extent, but leads to a disordered structure owing to the salting-out effect of POM if the prehydrolysis time is not long enough. Increased aging temperature is favorable for the formation of ordered mesostructures. However, hydrolysis of Si–O–W bonds and consequent removal of SiW_{11} from the silica framework also occur at such temperatures. Finally, the chemical linkage between the POM and the surface of mesoporous silica is further confirmed by the higher stability of the hybrid materials in water-leaching experiments compared to the impregnated samples, suggesting that the hybrid materials and the strategy for synthesizing these materials are significant for the acquisition of supported POM catalysts of high efficiency and practicability in applications using polar solvents as media.

1. Introduction

The study of functionalized ordered mesoporous silica materials has attracted much attention in the past decade due to their promising applications in adsorption, separation, catalysis, sensing, optics and other fields. As a method of immobilization of functional moieties on mesoporous silica, the surface functionalization technique has introduced a wide variety of organic functionalities, such as functional groups,[1–9] ligands,[10–13] polymers[14,15] and supermolecule compounds,[16–20] into the interior of mesopore channels through covalent linkage between functional moieties and the silica framework, greatly enriching the surface modification chemistry of mesoporous materials. Two approaches, grafting (post-synthesis)[1–5,10,11,14,16–18] and co-condensation (one-step synthesis)[6–9,12,13,15,19,20] have been developed as main functionalization strategies. Compared to grafting, the co-condensation synthesis is a more convenient route where organosilane is hydrolytically condensed together with conventional silica sources such as tetramethoxysilane (TMOS) and tetraethoxysilane (TEOS), and often endows the materials with larger pore sizes without pore blockages, and homogeneous distribution of the functional groups in the channels.[21]

Although these methods have made rapid progress in recent years resulting in the development of various functions, almost all of the introduction and immobilization of functionalities involve silanization reactions of surfaces with organosilanes containing the functional moieties, or grafting of organosilanes at least at the first step as a bridge for the introduction of functionalities. Few direct connections of functional groups, especially inorganic species, to silica surfaces have been reported.[22–24] Thus, functionalized mesoporous silica materials are also often called "organic–inorganic hybrid materials". To our knowledge, ordered mesoporous materials modified directly by bulky inorganic species through chemical bonding have not yet been reported.

Polyoxometalates (POMs), inorganic metal–oxygen cluster compounds,[25] have received increasing interest owing to their applications in various fields, in particular in catalysis. They, especially the familiar Keggin-type POMs, have been widely used as acid catalysts, oxidation catalysts as well as bifunctional catalysts[26–28] and were also employed as effective photocatalysts in the oxidation of organics in recent years.[29–31] Heterogeneous catalyses using POMs have also been realized generally by

Jiangsu Key Laboratory of Biofunctional Materials, College of Chemistry and Environmental Science, Nanjing Normal University, Nanjing, 210097, P. R. China. E-mail: yangchun@njnu.edu.cn

† Electronic supplementary information (ESI) available: *t*-plots, DEPT 135 spectra, IR spectra, XRD patterns. See DOI: 10.1039/b800025e

dispersing them on solid supports in order to combine the properties of both the polyoxometalates and a high surface area support. Periodic ordered mesoporous materials are excellent candidates as supports because of their high surface areas and regular channels of uniform pore sizes in the mesoporous region (2–50 nm). Some mesoporous silica-supported heteropoly acids and their salts have shown high catalytic activity and shape selectivity especially for conversion and formation of large organic molecules.[32–34]

However, like most of the supported POM catalysts, mesoporous silica-supported POMs were usually prepared by impregnation or sol–gel inclusion.[33–40] Since no strong chemical linkage existed between the supports and the POMs, the POMs were easily leached from the surface in applications using polar solvents as media[35,39,40] or migrated to aggregate on the outer surface of the support when water was formed as a side-product in the reaction.[36] The extraction of POMs included within pore walls also led to collapse of the walls and destruction of the mesostructure.[38] A few efforts were made to immobilize POMs on mesoporous MCM-41,[41,42] SBA-15,[43] MCF,[43] and SiO_2 xerogel[43,44] by electrostatic interaction or on macroporous, mesoporous and amorphous silica by dative bonding[45] *via* a post-synthesis route, in which organosilanes were used as bridges for attaching POMs. Another creative study was done by Stein's group.[46] They incorporated divacant γ-SiW_{10} clusters into macroporous silica *via* a sol–gel process as well as a latex sphere templating technique. In the synthesis, POM was connected with the silica wall by covalent bonding with or without organosilane bridges. An extended work with monovacant XW_{11} (X = P, Si, Ge, B) was also performed successively by Guo *et al.*[47] However, no covalent binding established between POMs and the ordered mesoporous materials by using a similar POM precursor has been reported up to now, because the synthesis of materials templated by surfactant micelles and the construction of periodic mesopores are more complex and more difficult, in which different synthetic conditions are required according to the silicon source and surfactant, POM species may be unstable or unable to react with the surface under such conditions. Additionally, the introduction of bulky POMs may be unfavorable for the assembly of surfactant micelles so that no ordered mesostructure is formed in the synthesis. Therefore, whether from the viewpoint of exploring a new synthesis strategy of POM-functionalized ordered mesoporous materials or from that of fixing POMs on mesoporous materials by chemical linkage, it is an interesting challenge to anchor POMs onto the periodic ordered mesoporous silica directly by covalent bonding.

In the present paper, we proposed a route partially similar to Stein's for covalently anchoring POMs on mesoporous silica, by which a POM-functionalized hybrid material of regular ordered mesopores was synthesized for the first time. In this route, a Keggin-type monovacant polyoxometalate, $SiW_{11}O_{39}^{8-}$ (SiW_{11}), was used as a precursor of POM, and the co-condensation approach was employed in the presence of block copolymer $EO_{20}PO_{70}EO_{20}$ (P123). The state and structure of POM in the hybrid material were characterized, and the synthetic conditions and conversion process were investigated and discussed in detail. From these, the synthesis scheme and the structure of the new material can be well understood. Finally, the stability of the hybrid materials against water-leaching was examined.

2. Experimental

2.1 Syntheses of polyoxometalate compounds

The TMA salt of $SiW_{12}O_{40}^{4-}$ (SiW_{12}) was prepared by precipitation with tetramethylammonium chloride (TMACl) in aqueous solution of $H_4SiW_{12}O_{40}\cdot nH_2O$. The potassium salt of $SiW_{11}O_{39}^{8-}$ (SiW_{11}) was synthesized using the procedure reported by Tézé and Hervé.[48] These compounds were checked by IR (see Fig. 1a and b).

The compound $SiW_{11}O_{39}[O(SiOH)_2]^{4-}$ ($SiW_{11}Si_2$) was synthesized by following a procedure reported for the synthesis of $SiW_{11}O_{39}[O(SiR)_2]^{4-}$ in ref. 49. It can be described in detail as follows. The potassium salt of SiW_{11} (4 g, 1.25×10^{-3} mol) was dissolved in water (100 mL). TEOS (0.99 g, 4.76×10^{-3} mol) was added dropwise with vigorous stirring. When the emulsion was dispersed, the pH was adjusted to 1 with 1 M HCl solution. After the mixture was stirred for 20 h, a clear solution was obtained. This solution was treated by different procedures depending on the nature of the cation. Potassium salt was obtained by drying this solution with a rotovapor, then purified by dissolution in water, filtering and drying again. After repeating the purification several times, the product was collected. Tetramethylammonium (TMA) salt and tetrabutylammonium (TBA) salt were obtained by adding TMACl and TBABr to the solution, respectively. The precipitates were collected by filtration and washed with isopropanol to remove SiO_n oligomers possibly formed in the reaction. IR, UV-vis/DRS and DEPT 135 spectra of the products are given in Fig. 1c, Fig. 2a, Fig. 3a and ESI† Fig. S3, respectively. Elemental analysis performed on the TBA salt was consistent with the formula $[Bu_4N]_4SiW_{11}O_{39}[O(SiOH)_2]$ (found: C, 20.4; H, 4.0; N, 1.7; W, 53.8; Si, 2.3%; calc: C, 20.5; H, 3.9; N, 1.5; W, 53.9; Si, 2.25%).

2.2 Syntheses of mesoporous hybrid silicas SiW_{11}/MHS

The mesoporous hybrid silicas SiW_{11}/MHS were synthesized according to ref. 50 and 51. In a typical preparation, 1 g of Pluronic P123 (Aldrich) was dissolved in 30 mL of 2 M HCl

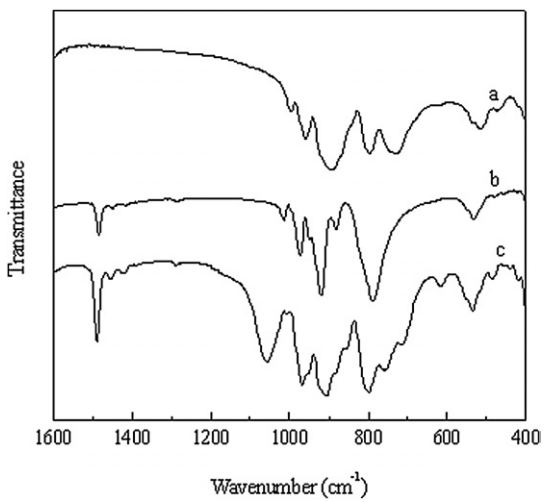

Fig. 1 IR spectra of (a) SiW_{11} (potassium salt), (b) SiW_{12} (TMA salt), (c) $SiW_{11}Si_2$ (TMA salt).

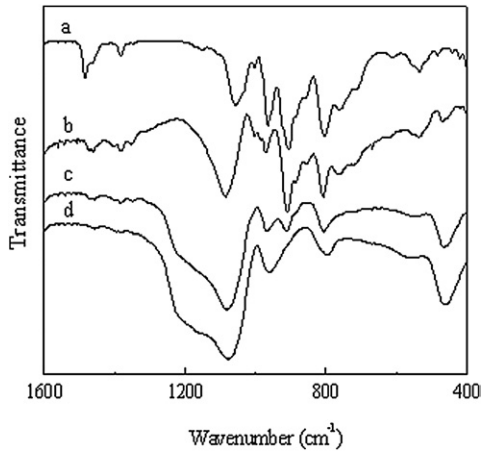

Fig. 2 IR spectra of (a) $SiW_{11}Si_2$ (TBA salt), (b) subtracting (d) from (c), (c) 5%SiW_{11}/MHS and (d) pure SBA-15. Aging temperature for (c) and (d) was 80 °C. Prehydrolysis time for (c) was 2 h.

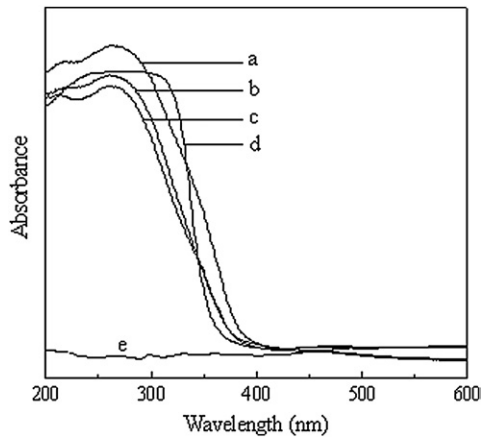

Fig. 3 UV-vis/DRS spectra of (a) $SiW_{11}Si_2$ (TBA salt), (b) 5%SiW_{11}/MHS, (c) 1.25% SiW_{11}/MHS, (d) SiW_{11} (potassium salt) and (e) pure SBA-15. Aging temperature for (b), (c) and (e) was 80 °C. Prehydrolysis time for (b) and (c) was 2 h.

solution with stirring at 40 °C. Then 2.1 g of TEOS were added into the solution. After stirring at 40 °C for a period of prehydrolysis of TEOS, the potassium salt of SiW_{11} (solid) and 7.5 mL of H_2O were added. The molar composition of the mixture for 1 g of copolymer was $(0.01 - x)$TEOS : $x$$SiW_{11}$: 0.06HCl : 1.96H_2O, where $x = 0.000125$ (1.25%), 0.00025 (2.5%), 0.0005 (5%), 0.00075 (7.5%), and 0.0010 (10%), corresponding to 0.41, 0.82, 1.63, 2.42 and 3.27 g of SiW_{11} in mass, respectively. The numbers in parentheses indicate the molar percentages of SiW_{11} in the initial mixture (TEOS + SiW_{11}) and are used to designate the samples. The resultant mixture was crystallized under stirring for an additional 24 h at 40 °C, and subsequently aged at a certain temperature for 24 h under static conditions. After cooling to room temperature, the solid product was recovered by filtration, washed thoroughly with water, and air-dried at room temperature overnight. The template was removed from the as-synthesized material by extraction with ethanol in a Soxhlet extractor for 36 h.

During the synthesis, the intermediates were investigated by IR. The POM species in the filtrate and elution liquid were detected with TMACl or TBABr, followed by IR measurement if a precipitate was obtained.

All chemical reagents used were analytical grade.

2.3 Preparation of impregnated samples and investigation of stability against water-leaching

The impregnated samples ($H_4SiW_{12}O_{40}$/SBA-15 and $K_4SiW_{11}O_{39}[O(SiOH)_2]$/SBA-15) were prepared by suspending 0.15 g of SBA-15 powder in aqueous solutions of 0.06 g of $H_4SiW_{12}O_{40}$ and $K_4SiW_{11}O_{39}[O(SiOH)_2]$, respectively. The slurry was stirred for 2 h and then the solvent was evaporated slowly at 60–80 °C. The content of $H_4SiW_{12}O_{40}$ or $K_4SiW_{11}O_{39}[O(SiOH)_2]$ in the impregnated sample (mol g^{-1}) was close to that of SiW_{11} in the hybrid sample 5%SiW_{11}/MHS.

The solubilities of the hybrid samples and the impregnated samples in water was investigated by washing them with water at a given temperature for 0.5–5 h (0.01g of solid sample per 40 mL of water). The solid sample was collected by filtration, and the filtrate was collected for elemental analysis to determine the percentage of POM lost in the leaching

2.4 Characterization

Powder X-ray diffraction (XRD) patterns of the samples were recorded on an ARL X'TRA diffractometer using Cu Kα radiation in the 2θ range from 0.5° to 6° (for small angle) or from 5° to 60° (for broad angle). Infrared (IR) spectra were collected on a Tensor-27 FTIR spectrometer with a resolution of 4 cm^{-1}. Samples were prepared as KBr pellets. UV-vis diffuse reflectance spectra (UV-vis/DRS) were recorded on a Varian Cary 5000 spectrophotometer using $BaSO_4$ as a reference. Transmission electron microscopy (TEM) micrographs were obtained on a JEOL JEM-2100 electron microscope operating at 200 kV. Elemental analyses for W, Si, K and Na were performed on a Leeman Lab Prodigy inductively coupled plasma-atomic emission spectroscopy (ICP-AES) instrument; analyses for C, H and N were carried out on an Elementar Vario EL III instrument. DEPT 135 spectra of TMA salts of $SiW_{11}O_{39}[O(SiOH)_2]^{4-}$ were obtained on a Bruker AV-400 spectrometer using dimethylsulfoxide (DMSO) as a solvent. Solid-state ^{29}Si CP MAS NMR measurements were performed on a Bruker AV-400 spectrometer operating at ^{29}Si frequency of 79.457 MHz and ^{1}H frequency of 399.952 MHz with the following conditions: magic angle spinning at 4 kHz; $\pi/2$ pulse; 3 s repetition delay. The chemical shifts were referenced to $(Me)_3Si(CH_2)_3SO_3Na$ external standard.

N_2 adsorption–desorption isotherms at 77K were measured using a Micromeritics ASAP 2020M physisorption analyzer. The samples were outgassed under vacuum at 120 °C for 6 h before the measurement. Surface area was calculated from adsorption data in the relative pressure range from 0.06 to 0.2 using the standard BET method. Mesopore diameter and mesopore size distribution were evaluated from the adsorption branch of the isotherm using the BJH model. Total pore volume was taken at the $P/P_0 = 0.98$ single point. Micropore volume was estimated by the t-plot method in the t range from 0.35 to 0.65 nm (see ESI,†

Fig. S1 and S2), applying the Harkins–Jura statistical film thickness equation with standard parameters obtained from a nonporous reference material. The micropore volumes of the disordered samples were not calculated.

3. Results and discussion

In the co-condensation approach, functional groups or ligands, usually contained in organosilane, are directly introduced and connected with the silica framework during the synthesis of mesoporous silica. In order to introduce a POM into the mesophase by co-condensation, two key problems should be considered. (1) Are there reactive sites on the surface of the POM by which the POM can condense easily with the silica precursor employed in the synthesis and bound onto the material during the construction of the mesoporous framework? (2) How can materials be acquired with both intact Keggin unit and regular mesostructure by controlling the synthesis conditions?

For the first problem, monovacant tungstosilicate $SiW_{11}O_{39}^{8-}$ (SiW_{11}), an unsaturated Keggin ($SiW_{12}O_{40}^{4-}$) fragment, can be considered as a precursor of POM for the synthesis, because oxygen atoms of sufficiently high nucleophilicity exist on its surface that it can act as a multidentate ligand or a nucleophilic reagent. It was reported that SiW_{11} could react with Si atoms of trialkoxysilane by a nucleophilic mechanism in an acidic medium of pH = 1 to yield its organic derivatives containing Si–O–W bonds, $SiW_{11}O_{39}[O(SiR)_2]^{4-}$.[49] In this reaction, two tetrahedral Si atoms were inserted into the vacancy of SiW_{11}, and a Si–O–Si bridge was formed between two Si atoms, thus the lacunary Keggin structure became saturated (see Scheme 1). According to the reported procedure, we made an analogous synthesis by replacing trialkoxysilane with TEOS to investigate the reactivity of SiW_{11} with TEOS, a Si precursor employed in the synthesis of mesoporous silica. A tetramethylammonium (TMA) salt, a tetrabutylammonium (TBA) salt and a potassium salt of the product were obtained. The IR spectrum of the product in the region of 1200–400 cm^{-1} (Fig. 1c), which exhibited the fingerprint features of POMs, shows that it is neither initial SiW_{11} (Fig. 1a), nor saturated SiW_{12} (Fig. 1b) formed from a conversion of SiW_{11} under the acidic conditions, but a new compound, $SiW_{11}O_{39}[O(SiOH)_2]^{4-}$ (designated as $SiW_{11}Si_2$). The consistency of its IR characteristics with those of $SiW_{11}O_{39}[O(SiR)_2]^{4-}$ reported in ref. 49 suggests that they possess similar structures. The saturated tendency of the structure is clearly seen from Fig. 1c as compared with the lacunary structure of SiW_{11} (Fig. 1a): (1) the asymmetrical stretching band for Si–O in the central SiO_4 unit shifts towards higher frequency (from ~890 cm^{-1} to ~905 cm^{-1}) accompanied by a narrowing of band width so that the asymmetrical stretching bands for W–O–W at ~882 cm^{-1} can be observed as in the saturated structure; (2) the deformation vibration band for Si–O in the central SiO_4 unit shifts from ~515 cm^{-1} to ~535 cm^{-1}; (3) the W–O–W asymmetrical stretching band at ~800 cm^{-1} does not split so severely as in SiW_{11}, and weaker bands at 755 cm^{-1} and 710 cm^{-1} are found only as shoulders of the ~800 cm^{-1} band. Moreover, a Si–O–Si stretching vibration band appears at ~1050 cm^{-1}, indicating the formation of a Si–O–Si bridge.

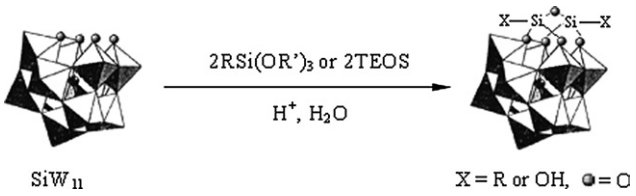

Scheme 1 Reaction of lacunary SiW_{11} cluster with siloxanes.

The DEPT 135 spectrum of TMA salt of $SiW_{11}O_{39}[O(SiOH)_2]^{4-}$ (see ESI,† Fig. S3) was also investigated. No lines are found except that for CH_3 in countercations, demonstrating that no CH_x groups are included in this anion, that is to say, the hydrolysis of TEOS is complete, and only SiOH groups are connected with oxygen atoms on the surface of the vacancy. Thus, the reaction of lacunary SiW_{11} with siloxanes can be depicted as in Scheme 1.

The synthesis of $SiW_{11}Si_2$ directly confirms the reactivity of lacunary POM toward TEOS, as revealed previously in the work of Stein *et al.*[46] and Guo *et al.*,[47] suggesting the feasibility of covalently grafting SiW_{11} onto mesoporous silica by co-condensation of SiW_{11} and TEOS under similar acidic conditions, which is available in the synthesis of mesostructured SBA-15. On the other hand, $SiW_{11}Si_2$ is an important reference compound useful in the characterization of hybrid materials. The direct evidence for covalent linkage of POMs on the silica surface can be obtained by a careful comparison of the hybrid samples with the compound (see below). Such evidence and arguments were not provided fully in the previous syntheses of POM-functionalized macroporous materials.[46,47]

As for the second problem mentioned above, various synthesis conditions have been investigated. It is found that the SiW_{11} content in the initial mixture, the temperature for aging the sample and the prehydrolysis time of TEOS are important factors which influence the quality of the product. From these experiments, we can obtain mesoporous hybrid silica materials, SiW_{11}/MHS, with both perfect Keggin units and regular mesoporous arrays under optimum conditions.

3.1 Synthesis and characterization of mesoporous hybrid silica SiW_{11}/MHS

The mesoporous hybrid silicas SiW_{11}/MHS were synthesized based on a sol–gel procedure, analogous to that published previously for SBA-15 silica[50,51] except for the addition of potassium salt of SiW_{11} as one of the inorganic precursors and the use of a TEOS prehydrolysis time prior to the addition of SiW_{11}. The samples were aged at a given temperature for one day after crystallization at 40 °C. The content of POM in the hybrid sample can be adjusted to a certain extent by changing the molar percentage of SiW_{11} in the initial mixture (TEOS + SiW_{11}). Elemental analyses for the solid hybrid sample, the filtrate and the ethanol extraction liquid indicate that only a portion of the initial SiW_{11} molecules are incorporated into the hybrid material, a considerable amount of POM molecules remain in the liquid phase and are lost during the filtration. Substitution of countercations of POM in the hybrid samples is also found by elemental analyses. Most of the K^+ ions imported from the potassium salt of SiW_{11} were replaced by H^+ in the acidic synthesis medium. After a thorough washing with deionized

water, soluble POM species, including free $SiW_{11}Si_2$ molecules and a small amount of SiW_{12} resulting from the conversion of SiW_{11} in the acidic medium, were removed from the hybrid samples. The template surfactant P123 was taken out subsequently from the as-synthesized materials by extraction with ethanol. Though P123 can also be removed by calcination at 450–500 °C, the POM was decomposed into SiO_2 and WO_3 at such temperatures as shown by the IR spectra of calcined samples (see ESI,† Fig. S4), and the sample colour changed to yellow-green from white.

The most important problem to us is whether the Si–O–W bond, *i.e.*, saturated $SiW_{11}Si_2$ structure is formed in the hybrid materials. This formation is a precondition of the establishment of covalent linkages between POM and the mesoporous silica framework. Thus, the characteristic IR absorption data, which are almost the most effective means to identify the structures of $SiW_{11}Si_2$ in the hybrid samples, were investigated carefully. It is seen from Fig. 2 that the features of saturated $SiW_{11}Si_2$ are present in the hybrid sample SiW_{11}/MHS (Fig. 2c). Although the Si–O–Si band (~1050 cm^{-1}) and W=O band (~960 cm^{-1}) for the $SiW_{11}Si_2$ structure are covered by the Si–O–Si band and Si–O band of mesoporous silica itself, respectively, an additional band is observed at ~910 cm^{-1} as compared to pure SBA-15 silica synthesized in an analogous way (Fig. 2d), and the intensity of the band increases with SiW_{11} loading. The band at ~800 cm^{-1} also becomes more intense and sharper owing to the absorption of the POM. Clearly, these bands result respectively from Si–O vibration of the central SiO_4 unit and W–O–W vibration in $SiW_{11}Si_2$ formed in SiW_{11}/MHS. A more explicit exhibition of the $SiW_{11}Si_2$ structure in the hybrid material is given in Fig. 2b, obtained by subtracting Fig. 2d from c. Almost all of the characteristic bands of $SiW_{11}Si_2$, rather than SiW_{11} or SiW_{12}, are shown clearly in Fig. 2b, denoting not only intact retention of the Keggin units of POM but also the formation of the $SiW_{11}Si_2$ structure in the hybrid materials.

UV-vis/DRS spectra of several samples are shown in Fig. 3. Unlike pure SBA-15 (Fig. 3e), all of the SiW_{11}/MHS samples exhibit UV absorption maxima at ~210 and ~265 nm (as shown in Fig. 3b and c), which are attributed to oxygen-to-tungsten charge transfer at W=O and W–O–W bonds of POM, respectively.[47] It is noticed that the UV absorption peaks of the hybrid materials are different from those of monovacant SiW_{11} (Fig. 3d) but similar to those of $SiW_{11}Si_2$ (Fig. 3a), indicating again the presence of saturated Keggin units in these materials.

The establishment of chemical linkage between the POM and the mesoporous silica can also be monitored by means of ^{29}Si CP MAS NMR (Fig. 4). Distinct resonances can be observed for various Si species in silica [$Q^n = Si(OSi)_n(OH)_{4-n}$, $n = 2$–4; Q^4 at −111 ppm, Q^3 at −102 ppm and Q^2 at −93 ppm]. The change of relative integrated intensities of Q^n signals after the introduction of SiW_{11} reflects the interconversion between these Si species during the incorporation. It can be seen from Fig. 4b that obvious increases in relative intensity of Q^4 and in Q^4/Q^n ($n = 2$, 3) integrated ratios occur when SiW_{11} is incorporated, implying the transformation of Q^2 and Q^3 species into Q^4 species owing to the formation of Si–O–Si bonds, which results from the condensation reaction of terminal SiOH groups in silica with $SiW_{11}Si_2$ species. An additional signal at −84.5 ppm attributed to the central SiO_4 unit in $SiW_{11}O_{39}[O(SiR)_2]^{4-}$[49] is also found in

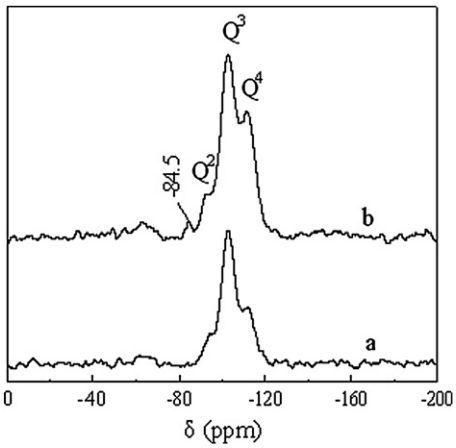

Fig. 4 ^{29}Si CP MAS NMR spectra of (a) pure SBA-15 and (b) 5%SiW_{11}/MHS. Aging temperature for (a) and (b) was 80 °C. Prehydrolysis time for (b) was 2 h.

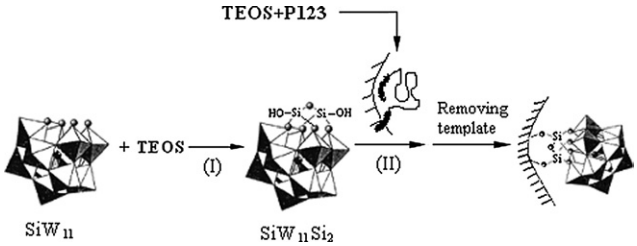

Scheme 2 Incorporation of SiW_{11} and bonding with the framework.

Fig. 4b, further suggesting the introduction of $SiW_{11}Si_2$ moieties onto the silica walls.

In view of the above characterization, we conclude that SiW_{11} can be incorporated onto the mesoporous silica framework according to Scheme 2. SiW_{11} reacts with TEOS to yield free $SiW_{11}Si_2$ molecules at step (I); then $SiW_{11}Si_2$ penetrate into the preorganized silica framework (inorganic–organic composite) and react with the framework by condensation between SiOH groups on both surfaces to block the terminal of silica at step (II). Thus, perfect Keggin units are linked covalently on the walls of mesoporous silica after removing the template. (More evidence for this scheme is given in section 3.2.) In fact, we have also successfully grafted a pre-prepared and isolated $SiW_{11}Si_2$ onto the surface of SBA-15 using a post-synthesis method (not discussed here). This gives obviously an additional argument to support Scheme 2.

The mesostructure of the hybrid materials can be characterized by small-angle powder XRD, TEM and N_2 adsorption–desorption measurements. Typical XRD patterns of the hybrid materials are shown in Fig. 5a and b. After the template surfactant is removed (Fig. 5b), the intensities of the diffraction peaks increase, and an intense peak (100), and weak peaks (110) and (200) appear in the range of $2\theta = 0.5$–6°, characteristic of an ordered hexagonal mesophase. However, the peak intensities of the hybrid sample are much lower than those of pure SBA-15 (Fig. 5c), indicating a partial loss of ordered mesostructure and a possible decrease of scattering contrast between the pore walls and the inside of pores because of the introduction of POM

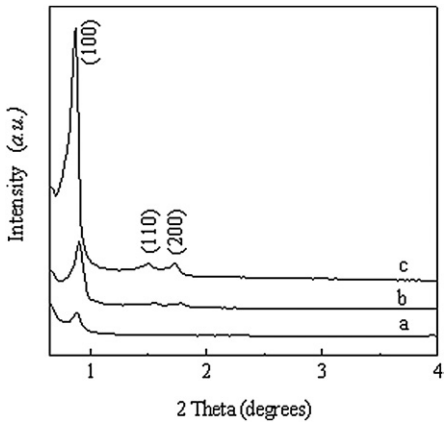

Fig. 5 XRD patterns of (a) 2.5%SiW_{11}/MHS before removing surfactant, (b) after removing surfactant and (c) pure SBA-15 after removing surfactant. Aging temperature for (a), (b) and (c) was 80 °C. Prehydrolysis time for (a) and (b) was 2 h.

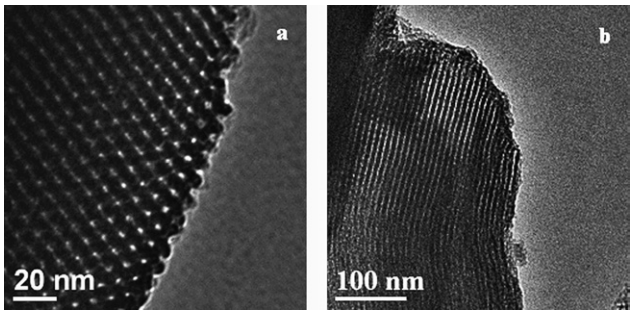

Fig. 6 TEM images of 5%SiW_{11}/MHS viewed along the pore axis (a) and perpendicular to the pore axis (b). Aging temperature and prehydrolysis time for the sample were 80 °C and 2 h, respectively.

molecules into the pores. The broad-angle XRD pattern of the hybrid sample (see ESI,† Fig. S5) shows no reflections of the POM crystal, suggesting a high dispersion of the POM species in the hybrid materials. Fig. 6 gives typical TEM images of the hybrid sample. An ordered hexagonal pore array can be seen. However, this mesoscopic ordered structure is slightly more difficult to observe on the hybrid samples, especially on those synthesized with higher SiW_{11} initial concentrations, than on pure SBA-15. Some disordered wormlike domains are also observed on the former samples.

Nitrogen adsorption–desorption measurements were used to study the textural properties of the hybrid samples. A typical isotherm and a pore size distribution for the hybrid sample are shown in Fig. 7. The type IV isotherms and type H1 hysteresis loops, characteristic of the SBA-15 architecture,[50] are presented. A steep capillary condensation step appearing at relative pressure of $P/P_0 = 0.6$–0.8 indicates the presence of regular mesopores in the samples, which is also confirmed by a narrow pore size distribution in the mesopore range (see inset in Fig.7). The pronounced change of N_2 adsorption–desorption data after the functionalization with POM is reflected in the pore parameters, as listed in Table 1 (*vide infra*). Decreases in specific surface areas and specific pore volumes compared with pure SBA-15 are observed, which may arise partially from the increase of specific

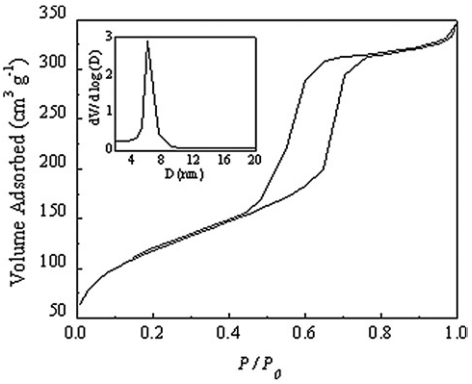

Fig. 7 N_2 adsorption–desorption isotherms and pore size distribution (inset) of 5%SiW_{11}/MHS. Aging temperature and prehydrolysis time for the sample were 80 °C and 2 h, respectively.

weights of the samples containing POM with large molecular mass. Of course, the loss of a section of ordered mesostructure should also be responsible for the change of pore parameter (*vide infra*).

3.2 Investigation of synthesis conditions and details in conversion

In the co-condensation approach, the incorporated molecules or groups may bring an unfavorable effect to the synthesis system and consequently to the final products depending on their size, mutual solubility with surfactant, acid–base properties and so on. The influence should be significant when a bulky inorganic salt is introduced into the system. Therefore, the choice and control of synthesis conditions to depress this effect is important for acquiring high quality mesoporous hybrid materials. On the other hand, an intensive study of the synthesis conditions will reveal some details of conversion during the synthesis, which is helpful to us to understand the mechanism of the synthesis. Among various conditions, the concentration of SiW_{11} in the initial mixture, the aging temperature and the prehydrolysis time of TEOS are found to be the most important factors.

An effective way to modify the loading of SiW_{11} in the hybrid material is altering the initial concentration of SiW_{11}, *i.e.*, molar ratio SiW_{11}/(TEOS + SiW_{11}) in the initial mixture. Fig. 8 shows the change of the contents of W and SiW_{11} (calculated on $SiW_{11}O_{39}$ basis) in the hybrid samples as a function of SiW_{11}/(TEOS + SiW_{11}) molar ratio. It can be seen that the loading of SiW_{11} increases with the increasing SiW_{11}/(TEOS + SiW_{11}) molar ratio when the concentration of SiW_{11} is lower; then the loading stabilizes at SiW_{11}/(TEOS + SiW_{11}) molar ratio $\geq$2.5%, suggesting a saturation of the amount of SiW_{11} chemically linked onto the mesoporous silica at a certain initial SiW_{11} concentration. Apparently, the utilization of SiW_{11} employed in the synthesis is lower than that of organosilane used in the synthesis of organically modified mesoporous materials by co-condensation. For the sample 5%SiW_{11}/MHS, elemental analyses indicate that the amount of SiW_{11} in the final solid product is only 22.5% of the total amount of SiW_{11} used, most of the POM (74.2%) is left in the liquid phase and lost during the washing and filtration. Moreover, a very small part (3.3%) is lost during the ethanol

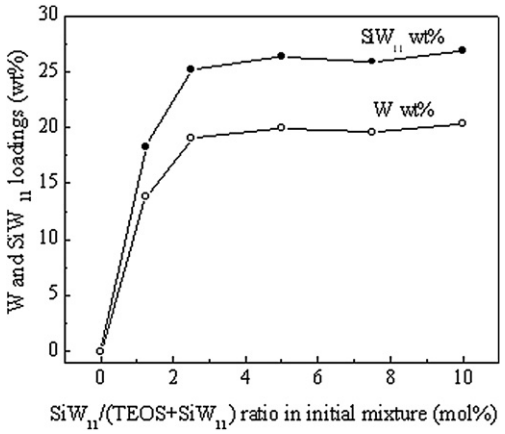

Fig. 8 Loadings of W and SiW_{11} in hybrid materials change as a function of molar fraction of SiW_{11} in inorganic precursors. Aging temperature and prehydrolysis time for the samples were 80 °C and 2 h, respectively.

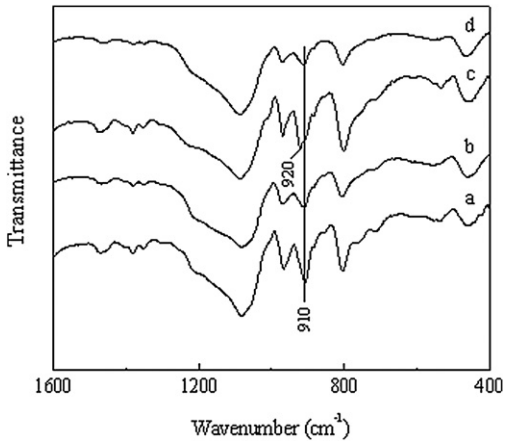

Fig. 9 IR spectra of the hybrid materials before and after aging at 80 °C. (a) 5%SiW_{11}/MHS unwashed before aging, (b) 5%SiW_{11}/MHS washed before aging, (c) 5%SiW_{11}/MHS unwashed after aging, (d) 5%SiW_{11}/MHS washed after aging. The prehydrolysis time for the samples was 2 h.

extraction. For the SBA-15 silica modified by organosilane (*e.g.* 3-mercaptopropyltrimethoxysilane), however, around 80–90% of organic species were incorporated by the co-condensation even though the molar ratio of organosilane in the initial mixture was higher (10–20%).[52] Similar incorporation degrees of organosilane were also observed in the cases where different structure-directing agents, such as CTAB,[53] and neutral surfactants, such as *n*-octylamine,[54] and alkylpoly(ethylene oxide)s[55] were employed. It can also be seen from Fig. 8 that W contents in all the samples are not more than 20 wt%, while that in the macroporous POM–SiO_2 hybrid materials prepared by Stein *et al.*[46] *via* a similar route was 28 wt%. The lower POM content in our samples may be caused by a more difficult penetration of SiW_{11} into the preorganized inorganic–organic composite than its incorporation into the inorganic SiO_2 network.

A detailed study on the intermediate and the POM species in the liquid phase can help us to understand how the POM are converted at different stages of the synthesis and when the saturation for incorporation occurs. When the synthesis of 5%SiW_{11}/MHS sample was interrupted after the crystallization at 40 °C without further aging, intense absorbance for $SiW_{11}Si_2$ species appeared in the IR spectrum of the product collected by filtration without washing (Fig. 9a). After thorough washing with water, the intensities of IR bands for $SiW_{11}Si_2$ species greatly decreased (Fig. 9b), indicating that a considerable amount of free $SiW_{11}Si_2$ molecules are included in the solid product and removed by washing. When the eluting liquid was detected with tetrabutylammonium bromide (TBABr), a white precipitate resulted which was collected. The IR spectrum showed that most of the precipitate was TBA salts of $SiW_{11}Si_2$, in which a small amount of TBA salts of SiW_{12} was also included. However, when the synthesis was continued with aging at 80 °C, the IR spectrum of the product (Fig. 9c) showed a decline of $SiW_{11}Si_2$ signals and a notable presence of a ~920 cm^{-1} band characteristic of SiW_{12}. After subsequent thorough washing with water, the ~920 cm^{-1} band disappeared and only $SiW_{11}Si_2$ species were observed in the IR spectrum (Fig. 9d). The intensities of $SiW_{11}Si_2$ bands in Fig. 9d are comparable with those of the unaged sample (see Fig. 9b). Similarly, the detection of the eluting liquid was performed with TBABr as well as IR spectra of TBA salts obtained, and a great increase in the amount of SiW_{12} in the liquid phase was found. These transformations of the products and the species in the liquid phase before and after aging suggest the following: (1) most of the SiW_{11} molecules react firstly with TEOS to form the free $SiW_{11}Si_2$ compounds when they are introduced into the synthesis system as shown in step (I) in Scheme 2, except that a small amount of SiW_{11} is converted to SiW_{12} in the acidic medium. The reaction of step (I) is easy; but step (II), *i.e.*, the reaction of $SiW_{11}Si_2$ with the preorganized inorganic–organic composite, is difficult so that many $SiW_{11}Si_2$ species remain as free molecules and are removed by washing. This phenomenon may be related to the fact that the bulky POM molecules penetrate into the interior of the preorganized inorganic–organic composite less easily than do the small organosilanes, thus limiting their incorporation. (2) An elevated temperature is unfavorable for the formation of $SiW_{11}Si_2$ species, and converts them to SiW_{12} efficiently. For the temperature of 80 °C, this conversion involves mostly the free $SiW_{11}Si_2$ molecules, while $SiW_{11}Si_2$ species bound on the silica framework are not influenced significantly, as shown by the comparable IR intensities of $SiW_{11}Si_2$ species in the samples washed before and after aging, suggestingg that the linked $SiW_{11}Si_2$ species are more stable than those free molecules in the solution.

When the concentration of SiW_{11} in the initial mixture was reduced to SiW_{11}/(TEOS + SiW_{11}) molar ratio = 2.5%, not only were the SiW_{12} species hardly detected by TBABr, but also the free $SiW_{11}Si_2$ molecules in the system decreased significantly, meaning that the utilization of SiW_{11} was enhanced at a lower SiW_{11} initial concentration. This also suggests again that SiW_{11} react primarily with unpolymerized TEOS remaining in solution, and are converted to SiW_{12} only when their amount is in excess relative to the remaining TEOS.

When the temperature for aging was further increased, however, not only did the decomposition of free $SiW_{11}Si_2$ molecules take place but also the removal of $SiW_{11}Si_2$ species linked on silica from the framework was observed by IR measurement (Fig. 10). In Fig. 10d, the ~910 cm^{-1} band characteristic of $SiW_{11}Si_2$ species weakens at 100 °C, although it is

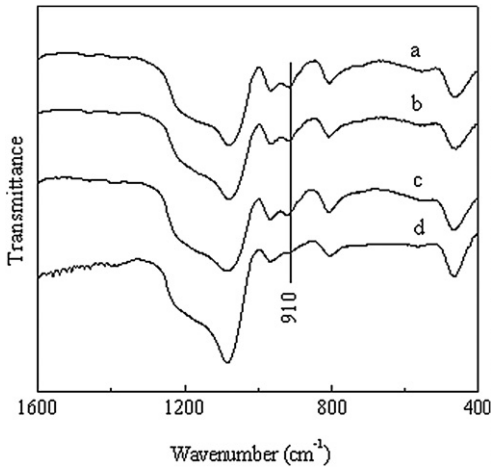

Fig. 10 IR spectra of 2.5%SiW_{11}/MHS synthesized at different aging temperatures: (a) 40 °C, (b) 60 °C, (c) 80 °C, and (d) 100 °C. The prehydrolysis time for the samples was 2 h.

held from 40 °C to 80 °C, indicating that even the bound species were also decomposed at higher temperature.

In order to confirm the effect of high temperature, a modified synthesis of $SiW_{11}Si_2$ was carried out as follows: After the reaction was performed at room temperature for 24 h, the solution was heated to 80 °C and maintained at that temperature for an additional 24 h rather than being treated immediately as described in the Experimental section, and then the product was precipitated out with tetramethylammonium chloride (TMACl). It was found that the product was SiW_{12} instead of $SiW_{11}Si_2$ (see Fig. 11a), similar to the phenomenon mentioned above occurring for the hybrid sample aged at 80 °C. Furthermore, a control experiment was performed for the synthesis of the hybrid material with SiW_{11}/(TEOS + SiW_{11}) molar ratio = 5% and a prehydrolysis time of 2 h: all procedures were preserved consistently with those in the conventional synthesis but there was no addition of P123 into the initial mixture. It was noticed that no solid

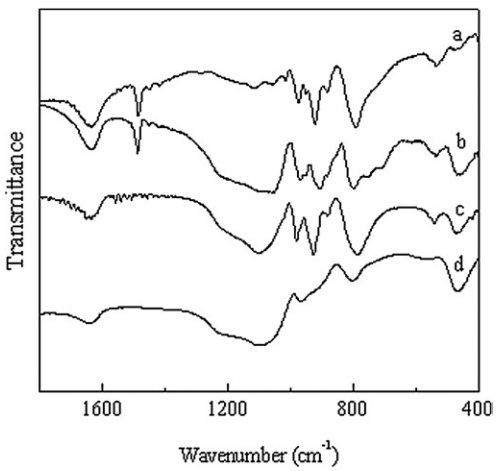

Fig. 11 IR spectra of (a) the product obtained after aging synthetic mixture of $SiW_{11}Si_2$ at 80 °C, (b) the precipitate obtained by adding TMACl before aged at 80 °C in control experiment, (c) the product obtained after aged at 80 °C in control experiment, (d) the product obtained after washing (c) with H_2O.

was produced after the crystallization at 40 °C for 26 h and a clear solution was obtained, different from that in the conventional synthesis in which a silica precipitate appeared during the crystallization. A part of this solution was taken and the product was precipitated out with TMACl. The rest of the solution was further aged at 80 °C for 24 h and then a SiO_2 gel was obtained, which was dried at 60 °C in vacuum and washed with water. The IR spectra of products obtained in each step are shown in Fig. 11b–d. Clearly, $SiW_{11}Si_2$ species had formed in the solution before the system underwent the ageing (Fig. 11b). The broad and intense Si–O–Si stretching band (~1080 cm^{-1}) indicates a synchronous formation of polymeric SiO_2, which connected $SiW_{11}Si_2$ species and was isolated together with $SiW_{11}Si_2$ by precipitation with TMACl. However, $SiW_{11}Si_2$ species were absent and the POM species were converted to SiW_{12} after the system was aged at 80 °C (Fig. 11c). After the sample was washed with water (Fig. 11d), the POM disappeared almost completely and only amorphous silica remained, *i.e.*, the formed SiW_{12} species were adsorbed or included in the sample rather than bound with the framework and can be removed by washing.

Based on the above experiment, we speculate that the hydrolysis of Si–O–W bonds in $SiW_{11}Si_2$ units in the hybrid material occurs at elevated temperature and two SiOH groups previously inserted into the vacancy are detached from the Keggin structure, thus $SiW_{11}Si_2$ are returned to SiW_{11} and removed from the SiO_2 framework. In the acidic medium (pH = 1), the removed SiW_{11} is converted to SiW_{12} as described in Scheme 3.

Although $SiW_{11}Si_2$ species in amorphous silica were hydrolyzed and removed almost fully at elevated temperature because of their poor stability, some $SiW_{11}Si_2$ species were still retained in the hybrid materials even after aging at the same temperature (compare Fig. 11d with Fig. 9d), suggesting that the phase separation at lower temperature and the inorganic–organic assembly have a certain protection effect on $SiW_{11}Si_2$ species in the hybrid materials. We noticed that, in the control experiment, no silica precipitate was formed during the crystallization at 40 °C, *i.e.*, $SiW_{11}Si_2$ species linked with the silica network remained in the solution and were attacked more easily by water at elevated temperature. In the synthesis of the hybrid materials, however, silica solid was formed even at 40 °C. The isolated silica phase and the inorganic–organic assembly structure may be unfavorable for the access of water to $SiW_{11}Si_2$ species for hydrolysis, leading to the remains of $SiW_{11}Si_2$ bound with the silica framework.

The small-angle powder XRD patterns of the samples synthesized using different initial SiW_{11} concentrations and aged at different temperatures are shown in Fig. 12A and B,

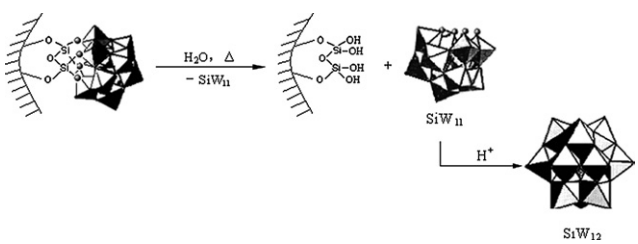

Scheme 3 Hydrolysis of $SiW_{11}Si_2$ and removal of SiW_{11}.

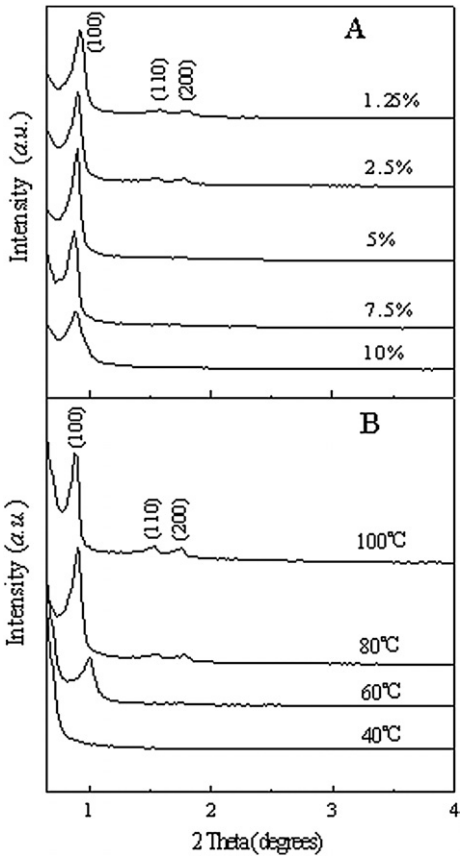

Fig. 12 XRD patterns of the hybrid samples synthesized using different initial SiW_{11} concentrations (A) and aged at different temperatures (B). The aging temperature for the samples in (A) was 80 °C. The initial SiW_{11} concentration for the samples in (B) was 2.5%. The prehydrolysis time for all the samples was 2 h.

respectively. The hexagonal symmetry can be observed for the most of hybrid samples with different initial SiW_{11} concentrations, as evidenced by their intense diffraction peaks of (100) (see Fig. 12A). The higher order (110) and (200) reflections are also seen clearly for the samples with lower SiW_{11}/(TEOS + SiW_{11}) ratio, but diminish in intensity or disappear entirely as the initial SiW_{11} concentration is increased. For the sample of SiW_{11}/(TEOS + SiW_{11}) = 10%, even peak (100) becomes weak and broad, implying the reduction of long-range order of the mesophase and the increase of the disordered or amorphous component with increasing SiW_{11} concentration, in agreement with the results reported by other authors in syntheses of organosilica mesophases with MCM-41,[53] MSU,[55] and SBA-15-type[52] architectures. This is apparently caused by the perturbation of an elevated concentration of SiW_{11} on the formation and self-assembly of surfactant aggregates. Compared with the initial SiW_{11} concentration, the aging temperature shows a more significant effect on the mesostructures of the samples. It can be seen from Fig. 12B that amorphous or less ordered samples are obtained when the aging temperature is lower than 80 °C; higher aging temperature is necessary to acquire SiW_{11}/MHS hybrid material with long-range ordered mesostructure, although such temperatures are unfavorable for the formation of chemical bonds between SiW_{11} and mesoporous silica.

The N_2 adsorption–desorption data for various samples are summarized in Table 1. The appearances and shapes of N_2 adsorption–desorption isotherms for the samples with different initial SiW_{11} concentrations are similar, but the surface areas and the total pore volumes gradually decrease as the SiW_{11} concentration is increased, which should be attributed to the increase in specific weights of the samples and in content of the disordered components, as mentioned above. A decrease in pore sizes with increasing molar SiW_{11} ratios is also observed, suggesting an enhanced density of the POM on the pore wall, which is supported by the increasing wall thickness. In addition, lower surface areas and pore volumes are shown for the samples obtained at lower aging temperatures because the mesoscopically ordered texture is not formed at such temperatures.

The presence of a significant amount of disordered micropores and small mesopores with the size below 3 nm within the wall of primary mesopores of SBA-15 has been confirmed.[56–60] These complementary pores are developed during the synthesis as a result of the penetration of poly(ethylene oxide) chains of the P123 template into the pore wall of SBA-15, and their volumes can be evaluated using the α_s-plot or t-plot methods.[56,57,59,60] We expect that the properties of the complementary pores may be varied after the POM is introduced and calculated the micropore volumes of the hybrid materials from t-plots of N_2 adsorption data (see Table 1). Similar to the total pore volumes, the

Table 1 Structure parameters of synthesized samples[a]

Sample[b]	T/°C	a_0/nm	D/nm	L/nm	S_{BET}/m^2 g^{-1}	V_t/mL g^{-1}	V_{mi}/mL g^{-1}
SBA-15	80	11.6	7.4	4.2	892	0.99	0.106
1.25%SiW_{11}/MHS	80	11.1	6.9	4.2	589	0.70	0.076
2.5%SiW_{11}/MHS	80	11.3	7.1	4.2	509	0.65	0.048
5%SiW_{11}/MHS	80	11.3	6.1	5.2	429	0.52	0.028
7.5%SiW_{11}/MHS	80	11.6	6.1	5.5	366	0.47	0.002
10%SiW_{11}/MHS	80	11.6	6.0	5.6	294	0.36	[c]
2.5%SiW_{11}/MHS	40	—	—	—	244	0.13	—
2.5%SiW_{11}/MHS	60	10.2	4.8	5.4	364	0.30	0.050
2.5%SiW_{11}/MHS	100	11.6	7.4	4.2	526	0.81	0.003

[a] T = aging temp., $a_0 = 2d_{100}/\sqrt{3}$ (d_{100}= (100) spacing), D = mesopore size calculated by the BJH method from the adsorption branch of the N_2 isotherm, L = wall thickness = $a_0 - D$, S_{BET} = surface area evaluated by the BET method, V_t = single point total pore volume, V_{mi} = micropore volume evaluated by the t-plot method (see ESI,† Fig. S1). [b] The samples were synthesized using a prehydrolysis time of 2 h. [c] V_{mi} cannot be well evaluated because the intercept of the ordinate in t-plot is below zero.

micropore volumes also decrease after the introduction of the POM due to the changes of specific weights of samples. For the samples with the molar SiW_{11} ratios $\geq$2.5%, however, the contribution from the specific weight should be neglected because actual loadings of SiW_{11} for these samples are comparable. Thus, the reduction in micropore volume may be attributed to filling and blockage of the micropores and small mesopores, including those in the disordered or amorphous component, by the Keggin units with a size of about 1.2 nm.[33b,38] As the molar SiW_{11} ratio increases, the ordered primary mesopores in the hybrid sample decrease; more POM molecules, which should be located at the primary mesopores, are bound into the micropores and small mesopores, leading to the blockage of these pores and the reduction of the micropore volume. The clogging of micropores was also observed in POM-functionalized macroporous materials prepared using similar POM precursors.[47] Moreover, the micropore volumes of the hybrid samples synthesized at different aging temperatures are also listed in Table 1. They decrease with increasing temperature despite the opposite change in total pore volume, in accordance with the reported dependence of micropore volume on the temperature.[56,57,60]

Another factor influencing the structures of SiW_{11}/MHS hybrid materials is the prehydrolysis time of TEOS, *i.e.*, the time for constructing and developing the silica framework wall solely by the hydrolysis and polymerization of TEOS around the template aggregates before the addition of the other precursor into the system. The necessity of the prehydrolysis time has been found in the synthesis of organically functionalized SBA-15 by co-condensation.[52,61] The premature introduction of the other precursor will perturb the assembly of surfactant aggregates, and thus disturb the formation of the ordered mesostructure. Therefore, giving enough time for the prehydrolysis of TEOS should be considered.

XRD patterns of 5%SiW_{11}/MHS synthesized using different prehydrolysis times are shown in Fig. 13A. It is seen that the ordered mesostructure is not obtained until the prehydrolysis time $\geq$1.25 h, and no notable modification in structure order is observed when the prehydrolysis time is further prolonged, evidencing that sufficient prehydrolysis time is necessary for the formation of ordered SiW_{11}/MHS mesoporous hybrid material, but longer prehydrolysis times do not contribute further to the order of the mesostructure. We observed that the white silica precipitate, *i.e.*, bulky visible SiO_2 polymer particles assembled around the template surfactant, appeared at 20–30 min after the addition of TEOS. The addition of SiW_{11} before that moment or not long after that moment influenced the assembly of preorganized inorganic–organic aggregates, resulting in a disordered structure or even an amorphous material. Accordingly, SiW_{11} should be introduced after the formation of a massive inorganic–organic aggregate, *i.e.*, surfactant aggregates surrounded by a thicker layer of silica, so that the assemblies of surfactant as well as the preorganized inorganic–organic aggregates are not perturbed by SiW_{11} owing to the protection of the thick SiO_2 layer.

However, how long a prehydrolysis time is needed depends on the concentration of SiW_{11} in the initial mixture. It is seen from XRD patterns in Fig. 13B that, when the SiW_{11}/(TEOS + SiW_{11}) molar ratio is lower (1.25%), the mesoscopic order of the sample

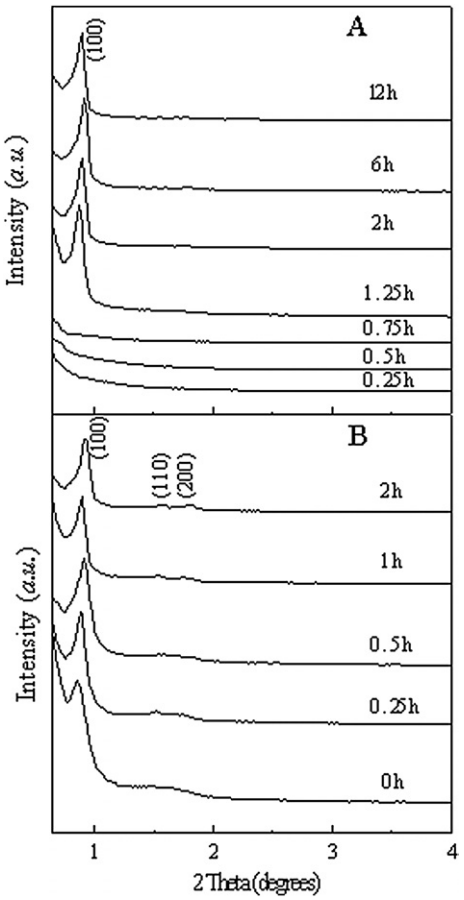

Fig. 13 XRD patterns of (A) 5%SiW_{11}/MHS and (B) 1.25%SiW_{11}/MHS synthesized using different prehydrolysis times and aged at 80 °C.

is not influenced even when the prehydrolysis time is decreased to 0 h. Apparently, the preorganized inorganic–organic aggregates are less perturbed when a lower concentration of SiW_{11} is employed in the synthesis.

The parameters for the textural properties of the samples synthesized with different prehydrolysis time and aged at 80 °C are summarized in Table 2. For the samples with the same initial SiW_{11} concentration, especially for 1.25%SiW_{11}/MHS with shorter investigated prehydrolysis times (0–2 h), the primary mesopore size and the total pore volume decrease with increasing prehydrolysis time, accompanied by the opposite trend in micropore volume. This phenomenon suggests that the employed prehydrolysis time may influence the location and distribution of the POM in the hybrid materials. At the initial stage of constructing the pore structure, more micropores/small mesopores are filled and blocked since the added SiW_{11} is embedded and bound into these pores more easily during the initial evolution of pores, while the primary channels are less occupied because they are built incompletely and fewer POM molecules can be located there. As the prehydrolysis time is prolonged, the construction of primary mesopore walls develops towards completion, SiW_{11} added at this stage enters the micropores/small mesopores, which have been filled by the poly(ethylene oxide) chains, less easily than it occupies the primary channels. Therefore, the smaller total pore volumes and primary mesopore sizes, as well as the

Table 2 Structure parameters of samples synthesized using different prehydrolysis times[a]

Sample[b]	PT/h	a_0/nm	D/nm	L/nm	S_{BET}/m^2 g^{-1}	V_t/mL g^{-1}	V_{mi}/mL g^{-1}
1.25%SiW_{11}/MHS	0	11.9	8.5	3.4	564	0.84	0.028
1.25%SiW_{11}/MHS	0.25	11.5	8.3	3.2	550	0.85	0.015
1.25%SiW_{11}/MHS	0.5	11.1	7.5	3.6	564	0.71	0.039
1.25%SiW_{11}/MHS	1	11.3	7.5	3.8	513	0.64	0.053
1.25%SiW_{11}/MHS	2	11.1	6.9	4.2	589	0.70	0.076
5%SiW_{11}/MHS	0.25	—	—	—	245	0.18	—
5%SiW_{11}/MHS	0.5	—	—	—	403	0.32	—
5%SiW_{11}/MHS	1.25	11.6	6.3	5.3	436	0.57	0
5%SiW_{11}/MHS	2	11.3	6.1	5.2	429	0.52	0.028
5%SiW_{11}/MHS	6	11.1	6.1	5.0	434	0.53	0.028
5%SiW_{11}/MHS	12	11.3	6.1	5.2	414	0.52	0.026

[a] PT = prehydrolysis time, $a_0 = 2d_{100}/\sqrt{3}$ (d_{100}= (100) spacing,), D = mesopore size calculated by the BJH method from the adsorption branch of the N_2 isotherm, L = wall thickness = $a_0 - D$, S_{BET} = surface area evaluated by the BET method, V_t = single point total pore volume, V_{mi} = micropore volume evaluated by the t-plot method (see ESI,† Fig. S2). [b] The samples were aged at 80 °C.

larger micropore volumes are observed at this stage. This indicates that SiW_{11} is chemically linked mostly on the surface of primary mesopores rather than in the complementary pores as long as the prehydrolysis time is long enough.

How does SiW_{11} perturb the formation and assembly of surfactant aggregates? We observed that, in the synthesis of the 5%SiW_{11}/MHS sample, the massive viscous solid was precipitated out from the solution as soon as SiW_{11} was added at 0.25 h prehydrolysis time (no solid was precipitated out at that moment if SiW_{11} was not added). The IR spectrum of the viscous solid shows a mixture of $SiW_{11}Si_2$, SiO_2 and P123 (see ESI,† Fig. S6), indicating that the added SiW_{11} not only reacts immediately with Si species to yield linked $SiW_{11}Si_2$–SiO_2 oligomers but also induces the isolation of viscous P123. A control experiment, in which the conventional procedures for the synthesis of the hybrid material were followed except for the addition of TEOS, also revealed that the dissolved P123 was isolated immediately when SiW_{11} was introduced. These facts suggest that SiW_{11} possesses the ability to reduce the solubility of the copolymer P123 in water, *i.e.*, salting-out effect, a prevalent phenomenon in the nonionic surfactant solution with salt addition.[62] This effect greatly diminishes the critical micelle concentration of P123 in water, causing a considerable amount of P123 to be congregated into larger micelles or isolated out as a solid. In such a perturbed system without ordered template assembly, TEOS is hydrolyzed and polymerized towards the disordered or amorphous material. This should be the main reason why the mesoscopic ordered hybrid materials can not be obtained at higher initial SiW_{11} concentration and shorter prehydrolysis time. Notably, the perturbation effect of POM on the assembly of P123 surfactant is much greater than that of organosilane, and is performed *via* a different mechanism.[52]

3.3 Stability of the SiW_{11}/MHS hybrid materials against water-leaching

In order to investigate the immobilized extent of the POM in the hybrid materials, we washed them with deionized water at a given temperature under stirring. IR spectra of the leached hybrid samples (5%SiW_{11}/MHS synthesized using a prehydrolysis time of 2 h and aged at 80 °C) are shown in Fig. 14. Less loss of the POM is observed at lower temperature, as shown by

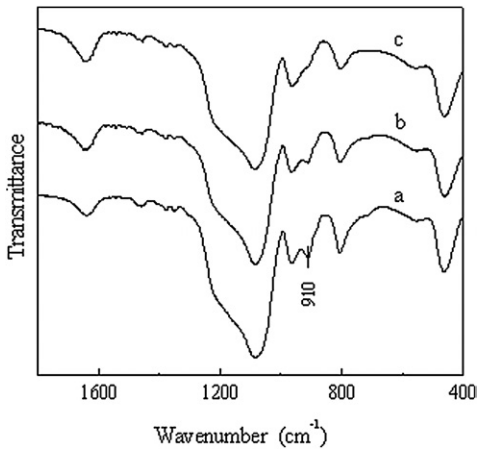

Fig. 14 IR spectra of 5%SiW_{11}/MHS leached with water for 5 h at 25 °C (a), 50 °C (b), and 80 °C (c).

the ~910 cm^{-1} band remaining in Fig. 14a and b. At an elevated temperature, however, the ~910 cm^{-1} band becomes dramatically weaker, indicating the removal of a number of POM, apparently caused by hydrolysis of $SiW_{11}Si_2$ bound on mesoporous silica. Furthermore, elemental analyses of leaching liquids were carried out and the percentage of the POM lost in leaching (loss (%)) was calculated by reference to the amount of POM in the samples before washing. As shown in Table 3, the loss of the hybrid samples increases with prolonged leaching time, especially with enhanced temperature; but they are still much lower than those of samples prepared by impregnating a similar amount of $H_4SiW_{12}O_{40}$ or $K_4SiW_{11}O_{39}[O(SiOH)_2]$ on pure SBA-15 owing to the chemical linkage between the POM and the silica framework. It can also be seen from Table 3 that the longer the prehydrolysis time used in synthesis, the more the POM molecules are removed from the sample during the leaching, supporting the conclusion mentioned above that the prehydrolysis time influences the distribution of POM in the hybrid materials, because the longer prehydrolysis time is favorable for the location of POM in the primary mesopores where water molecules access and hydrolyze them more easily.

Although a considerable amount of POMs were removed from the samples at elevated temperature, no destruction of the

Table 3 Data obtained from leaching experiments[a]

Sample	PT/h	Leaching temp./°C	Leaching time/h	Loss (%)
5%SiW_{11}/MHS (H.S.)	2	25	0.5	11.7
		25	1	17.5
		25	5	29.0
		80	5	68.2
5%SiW_{11}/MHS (H.S.)	1.25	80	5	59.5
5%SiW_{11}/MHS (H.S.)	6	80	5	80.5
5%SiW_{11}/MHS (H.S.)	12	80	5	84.0
$H_4SiW_{12}O_{40}$/SBA-15 (I.S.)	—	25	0.5	83.2
		25	5	93.7
$K_4SiW_{11}O_{39}[O(SiOH)_2]$/SBA-15 (I.S.)	—	25	1	95.3

[a] H.S.= hybrid sample, I.S.= impregnated sample, PT = prehydrolysis time, loss = percentage of POM lost in leaching.

ordered mesostructure was observed by XRD and TEM after the washing, suggesting that the POM species are bound on the surface instead of in the SiO_2 network of the walls even if some of them are entrapped into the small pores on the walls, because the removal of a large amount of POM included within the walls can result in collapse of the mesostructure, as reported by Nowińska *et al.*[38]

4. Conclusion

Novel POM-functionalized mesoporous hybrid silicas with hexagonal mesostructure can be synthesized directly with TEOS and Keggin-type monovacant SiW_{11} as precursors in the presence of block copolymers. Covalent bonding is established between SiW_{11} and the interior surface of ordered mesopores by the formation of Si–O–W bonds, leading to the immobilization of POM molecules on the mesoporous silica and higher stability against water-leaching at room temperature compared with impregnated samples. In this synthesis, $SiW_{11}Si_2$ molecule is an intermediate, by which the condensation between POM and silica species is realized. The introduced SiW_{11} is not only bound on the surface of the walls of primary mesopores, but also entrapped in the complementary pores on the walls, especially when higher SiW_{11} initial concentrations or shorter prehydrolysis times are used in the synthesis.

The SiW_{11} concentration in the initial mixture, the prehydrolysis time of TEOS and the temperature for aging are important factors influencing the composition and structure of the hybrid material. Increasing SiW_{11} concentration can enhance the loading of POM to a certain extent so that the content of SiW_{11} in the hybrid material can reach 26–27 wt%. Excess SiW_{11} in the initial mixture is unfavorable for the synthesis because they disturb the ordered structure of the product due to the salting-out effect on the surfactant. Prolonging the prehydrolysis time is a good method to suppress this effect when a higher initial SiW_{11} concentration is employed, but weak and local perturbation from SiW_{11} still exists in the system, so that a part of a disordered wormlike structure appears even if the prehydrolysis time is very long. The aging temperature influences not only the formation of the ordered hexagonal mesostructure, but also the loading of SiW_{11} because the hydrolysis of Si–O–W bonds occurs at elevated temperature. Considering a balance between both aspects, we recommend 80 °C as the optimal temperature for aging.

Acknowledgements

We thank the National Natural Science Foundation of China (20473037) for financial support.

References

1 (*a*) K. Y. Ho, G. McKay and K. L. Yeung, *Langmuir*, 2003, **19**, 3019; (*b*) C. Lei, Y. Shin, J. Liu and E. J. Ackerman, *J. Am. Chem. Soc.*, 2002, **124**, 11242.
2 (*a*) H. Yoshitake, T. Yokoi and T. Tatsumi, *Chem. Mater.*, 2002, **14**, 4603; (*b*) A. M. Liu, K. Hidajat, S. Kawi and D.-Y. Zhao, *Chem. Commun.*, 2000, 1145.
3 T. Kang, Y. Park, K. Choi, J. S. Lee and J. Yi, *J. Mater. Chem.*, 2004, **14**, 1043.
4 (*a*) D. Das, J-F. Lee and S. Cheng, *Chem. Commun.*, 2001, 2178; (*b*) D. Das, J.-F. Lee and S.-F. Cheng, *J. Catal.*, 2004, **223**, 152; (*c*) V. Dufaud and M. E. Davis, *J. Am. Chem. Soc.*, 2003, **125**, 9403.
5 (*a*) V. Antochshunk, O. Olkhovyk, M. Jaroniec, I.-S. Park and R. Ryoo, *Langmuir*, 2003, **19**, 3031; (*b*) V. Antochshunk and M. Jaroniec, *Chem. Commun.*, 2002, 258.
6 (*a*) R. I. Nooney, M. Kalyanaraman, G. Kennedy and E. J. Maginn, *Langmuir*, 2001, **17**, 528; (*b*) L. Zhang, W. Zhang, J. Shi, Z. Hua, Y. Li and J. Yan, *Chem. Commun.*, 2003, 210.
7 (*a*) H. H. P. Yiu, C. H. Botting, N. P. Botting and P. A. Wright, *Phys. Chem. Chem. Phys.*, 2001, **3**, 2983; (*b*) J. G. C. Shen, R. G. Herman and K. Klier, *J. Phys. Chem. B*, 2002, **106**, 9975.
8 (*a*) N. Liu, R. A. Assink and C. J. Brinker, *Chem. Commun.*, 2003, 307; (*b*) N. Liu, Z. Chen, D. R. Dunphy, Y.-B. Jiang, R. A. Assink and C. J. Brinker, *Angew. Chem., Int. Ed.*, 2003, **42**, 1731; (*c*) N. Lin, D. R. Dunphy, P. Atanassov, S. D. Bunge, Z. Chen, G. P. Lopéz, T. J. Boyle and C. J. Brinker, *Nano Lett.*, 2004, **4**, 551.
9 (*a*) R. J. P. Corriu, L. Datas, Y. Guari, A. Mehdi, C. Reyé and C. Thieuleux, *Chem. Commun.*, 2001, 763; (*b*) M. Kruk, T. Asefa, M. Jaroniec and G. A. Ozin, *J. Am. Chem. Soc.*, 2002, **124**, 6383; (*c*) S. Huh, H.-T. Chen, J. W. Wiench, M. Pruski and V. S.-Y. Lin, *J. Am. Chem. Soc.*, 2004, **126**, 1010; (*d*) W.-H. Zhang, X.-B. Liu, J.-H. Xiu, Z.-L. Hua, L.-X. Zhang, M. Robertson, J.-L. Shi, D.-S. Yan and J. D. Holmes, *Adv. Funct. Mater.*, 2004, **14**, 544.
10 (*a*) J. Evans, A. B. Zaki, M. Y. El-Sheikh and S. A. El-Safty, *J. Phys. Chem. B*, 2000, **104**, 10271; (*b*) C.-H. Lee, T.-S. Lin and C.-Y. Mou, *J. Phys. Chem. B*, 2003, **107**, 2543; (*c*) M. Jia, A. Seifert and W. R. Thiel, *Chem. Mater.*, 2003, **15**, 2174.
11 (*a*) C. D. Nunes, A. A. Valente, M. Phillinger, A. C. Fernandes, C. C. Romão, J. Rocha and I. S. Gonçalves, *J. Mater. Chem.*, 2002, **12**, 1735; (*b*) S. Gago, Y. Zhang, A. M. Santos, K. Köhler, F. E. Kühn, J. A. Fernandes, M. Pillinger, A. A. Valente, T. M. Santos, P. J. A. Ribeiro-Claro and I. S. Gonçalves, *Microporous Mesoporous Mater.*, 2004, **76**, 131.
12 (*a*) H. R. Li, J. Lin, L. S. Fu, J. F. Guo, Q. G. Meng, F. Y. Liu and H. J. Zhang, *Microporous Mesoporous Mater.*, 2002, **55**, 103; (*b*) M. Jia, A. Seifert, M. Berger, H. Giegengack, S. Schulze and W. R. Thiel, *Chem. Mater.*, 2004, **16**, 877.
13 (*a*) R. J. P. Corriu, A. Mehdi, C. Reyé and C. Thieuleux, *Chem. Mater.*, 2004, **16**, 159; (*b*) R. J. P. Corriu, A. Mehdi, C. Reyé, C. Thieuleux, A. Frenkel and A. Gibaud, *New J. Chem.*, 2004, **28**, 156; (*c*) R. J. P. Corriu, A. Mehdi, C. Reyé and C. Thieuleux, *Chem. Commun.*, 2002, 1382.
14 Q. Fu, G. V. R. Rao, L. K. Ista, Y. Wu, B. P. Andrzejewski, L. A. Sklar, T. L. Ward and G. P. López, *Adv. Mater.*, 2003, **15**, 1262.
15 X. Ji, J. E. Hampsey, Q. Hu, J. He, Z. Yang and Y. Lu, *Chem. Mater.*, 2003, **15**, 3656.
16 (*a*) T. Seçkin and A. Gültek, *J. Appl. Polym. Sci.*, 2003, **90**, 3905; (*b*) E. J. Acosta, C. S. Carr, E. E. Simanek and D. F. Shantz, *Adv. Mater.*, 2004, **16**, 985.
17 (*a*) H. Furukawa, T. Watanabe and K. Kuroda, *Chem. Commun.*, 2001, 2002; (*b*) S. Murata, H. Hata, T. Kimura, Y. Sugahara and K. Kuroda, *Langmuir*, 2000, **16**, 7106.

18 A. Fukuoka, K. Fujishima, M. Chiba, A. Yamagishi, S. Inagaki, Y. Fukushima and M. Ichikawa, *Catal. Lett.*, 2000, **68**, 241.
19 (*a*) R. Huq, L. Mercier and P. J. Kooyman, *Chem. Mater.*, 2001, **13**, 4512; (*b*) A. Bibby and L. Mercier, *Green Chem.*, 2003, **5**, 15.
20 C. Liu, N. Naismith, L. Fu and J. Economy, *Chem. Commun.*, 2003, 2472.
21 A. Vinu, K. Z. Hossain and K. Ariga, *J. Nanosci. Nanotechnol.*, 2005, **5**, 347.
22 M. Alvaro, A. Corma, D. Das, V. Fornés and H. García, *Chem. Commun.*, 2004, 956.
23 K. Yamamoto and T. Tatsumi, *Microporous Mesoporous Mater.*, 2001, **44-45**, 459.
24 Y. Inaki, Y. Kajita, H. Yoshida, K. Ito and T. Hattori, *Chem. Commun.*, 2001, 2358.
25 (*a*) M. T. Pope, *Heteropoly and Isopoly Oxometalates*, Springer-Verlag, New York, 1993; (*b*) *Polyoxometalate Chemistry From Topology* via *Self-Assembly to Applications*, ed. M. T. Pope and A. Müller, Kluwer Academic Publishers, Dordrecht, 2001.
26 (*a*) N. Mizuno and M. Misono, *Chem. Rev.*, 1998, **98**, 199; (*b*) I. V. Kozhevnikov, *Chem. Rev.*, 1998, **98**, 171.
27 T. Okuhara, N. Mizuno and M. Misono, *Appl. Catal. A*, 2001, **222**, 63.
28 (*a*) C. L. Hill, in *Comprehensive Coordination Chemistry II*, ed. A. G. Wedd, Elsevier Science, New York, 2004, vol. 4, p. 679; (*b*) R. Neumann, in *Modern Oxidation Methods*, ed. J.-E. Baeckvall, Wiley-VCH, Weinheim, 2004, p. 223.
29 (*a*) C. Hu, B. Yue and T. Yamase, *Appl. Catal. A*, 2000, **194–195**, 99; (*b*) Y. Guo, Y. Wang, C. Hu and E. Wang, *Chem. Mater.*, 2000, **11**, 3501.
30 B. Yue, Y. Zhou, J. Xu, Z. Wu, X. Zhang, Y. Zou and S. Jin, *Environ. Sci. Technol.*, 2002, **36**, 1325.
31 A. Molinari, R. Amadelli, A. Mazzacani, G. Sartori and A. Maldotti, *Langmuir*, 2002, **18**, 5400.
32 S. Choi, Y. Wang, Z. Nie, J. Liu and C. H. F. Peden, *Catal. Today*, 2000, **55**, 117.
33 (*a*) N. G. Kostova, A. A. Spojakina, K. Jiratova, O. Solcova, L. D. Dimitrov and L. A. Petrov, *Catal. Today*, 2001, **65**, 217; (*b*) T. Blasco, A. Corma, A. Martínez and P. Martínez-Escolano, *J. Catal.*, 1998, **177**, 306.
34 (*a*) I. V. Kozhevnikov, K. R. Kloetstra, A. Sinnema, H. W. Zandbergen and H. van Bekkum, *J. Mol. Catal. A*, 1996, **114**, 287; (*b*) I. V. Kozhevnikov, A. Sinnema, R. J. J. Jansen, K. Pamin and H. van Bekkum, *Catal. Lett.*, 1995, **30**, 241.
35 W. Chu, X. Yang, Y. Shan, X. Ye and Y. Wu, *Catal. Lett.*, 1996, **42**, 201.
36 M. J. Verhoef, P. J. Kooyman, J. A. Peters and H. van Bekkum, *Microporous Mesoporous Mater.*, 1999, **27**, 365.
37 (*a*) P. A. Jalil, M. A. Al-Daous, A.-R. A. Al-Arfaj, A. M. Al-Amer, J. Beltramini and S. A. I. Barri, *Appl. Catal. A*, 2001, **207**, 159; (*b*) W.-G. Kim, M.-W. Kim, J.-H. Kim and G. Seo, *Microporous Mesoporous Mater.*, 2003, **57**, 113; (*c*) A. Lapkin, B. Bozkaya, T. Mays, L. Borello, K. Edler and B. Crittenden, *Catal. Today*, 2003, **81**, 611.
38 K. Nowińska, R. Fórmaniak, W. Kaleta and A. Wącław, *Appl. Catal. A*, 2003, **256**, 115.
39 B. L. C. Passoni, F. J. Luna, M. Wallau, R. Buffon and U. Schuchardt, *J. Mol. Catal.*, 1998, **134**, 229.
40 K. Nowińska and W. Kaleta, *Appl. Catal. A*, 2000, **203**, 91.
41 W. Kaleta and K. Nowińska, *Chem. Commun.*, 2001, 535.
42 W. Xu, Q. Luo, H. Wang, L. C. Francesconi, R. E. Stark and D. L. Akins, *J. Phys. Chem. B*, 2003, **107**, 497.
43 N. V. Maksimchuk, M. S. Melgunov, Yu. A. Chesalov, J. Mrowiec-Białoń, A. B. Jarzębski and O. A. Kholdeeva, *J. Catal.*, 2007, **246**, 241.
44 O. A. Kholdeeva, M. P. Vanina, M. N. Timofeeva, R. I. Maksimovskaya, T. A. Trubitsina, M. S. Melgunov, E. B. Burgina, J. Mrowiec-Bialon, A. B. Jarzebski and C. L. Hill, *J. Catal.*, 2004, **226**, 363.
45 B. J. S. Johnson and A. Stein, *Inorg. Chem.*, 2001, **40**, 801.
46 R. C. Schroden, C. F. Blanford, B. J. Melde, B. J. S. Johnson and A. Stein, *Chem. Mater.*, 2001, **13**, 1074.
47 Y. Guo, Y. Yang, C. Hu, C. Guo, E. Wang, Y. Zou and S. Feng, *J. Mater. Chem.*, 2002, **12**, 3046.
48 A. Tézé and G. Hervé, *J. Inorg. Nucl. Chem.*, 1977, **39**, 999.
49 P. Judeinstein, C. Deprun and L. Nadjo, *J. Chem. Soc., Dalton Trans.*, 1991, 1991.
50 D.-Y. Zhao, J.-L. Feng, Q.-S. Huo, N. Melosh, G. H. Fredrickson, B. F. Chmelka and G. D. Stucky, *Science*, 1998, **279**, 548.
51 D.-Y. Zhao, Q.-S. Huo, J.-L. Feng, B. F. Chmelka and G. D. Stucky, *J. Am. Chem. Soc.*, 1998, **120**, 6024.
52 D. Margolese, J. A. Melero, S. C. Christiansen, B. F. Chmelka and G. D. Stucky, *Chem. Mater.*, 2000, **12**, 2448.
53 C. E. Fowler, S. L. Burkett and S. Mann, *Chem. Commun.*, 1997, 1769.
54 J. Brown, L. Mercier and T. J. Pinnavaia, *Chem. Commun.*, 1999, 69.
55 (*a*) R. Richer and L. Mercier, *Chem. Commun.*, 1998, 1775; (*b*) J. Brown, R. Richer and L. Mercier, *Microporous Mesoporous Mater.*, 2000, **37**, 41.
56 R. Ryoo, C. H. Ko, M. Kruk, V. Antochshuk and M. Jaroniec, *J. Phys. Chem. B*, 2000, **104**, 11465.
57 M. Kruk, M. Jaroniec, C. H. Ko and R. Ryoo, *Chem. Mater.*, 2000, **12**, 1961.
58 H. J. Shin, R. Ryoo, M. Kruk and M. Jaroniec, *Chem. Commun.*, 2001, 349.
59 R. van Grieken, G. Calleja, G. D. Stucky, J. A. Melero, R. A. García and J. Iglesias, *Langmuir*, 2003, **19**, 3966.
60 A. Galarneau, H. Cambon, F. D. Renzo, R. Ryoo, M. Choi and F. Fajula, *New J. Chem.*, 2003, **27**, 73.
61 J. A. Melero, G. D. Stucky, R. van Grieken and G. Morales, *J. Mater. Chem.*, 2002, **12**, 1664.
62 (*a*) M. J. Schick, *J. Colloid Sci.*, 1962, **17**, 801; (*b*) P. Mukerjee and C. C. Chan, *Langmuir*, 2002, **18**, 5375.